

Critical Instability and Friction Scaling of Fluid Flows through Pipes with Rough Inner Surfaces

Jianjun Tao*

State Key Laboratory of Turbulence and Complex Systems, CAPT, Department of Mechanics and Aerospace Engineering,
College of Engineering, Peking University, Beijing 100871, China

(Received 1 June 2009; published 28 December 2009)

It has been shown experimentally over nearly 80 years that surface fine roughness of circular pipes has a crucial effect on the natural transition to turbulence. In this Letter, a theoretical explanation is suggested for the roughness-induced instability. Once the nonlinear effect of roughness is introduced (through a pipe with fine corrugation surface), the mean velocity profile becomes unstable to three-dimensional, asymmetric, and helical traveling waves at moderate Reynolds numbers. The threshold of the aspect ratio or shape factor of the roughness element required to cause instability scales as Re^{-2} . Inspired by the current model, a scaling form is proposed and the scaled friction factor measurements in rough pipes collapse onto a universal curve.

DOI: 10.1103/PhysRevLett.103.264502

PACS numbers: 47.20.Ft, 47.27.Cn, 47.27.nf

The laminar-turbulent transition in pipe flows has been an open problem since the original experiments of Reynolds [1]. Since the linear stability theory fails to explain the instability, finite-amplitude disturbance must play a key role for the onset of turbulence. The most natural disturbance may be the wall roughness. Nikuradze's experimental data [2] illustrate clearly that pipe roughness has a dominant effect on the laminar-turbulence transition and the turbulent states. A corrugated surface may be the simplest model of a rough wall. Comparing with the extensive studies of corrugated channel flows [3–5], the corresponding research on corrugated pipe flows is quite rudimentary [6,7]. The two-dimensional (no variation in the azimuthal direction) instability in a corrugated circular pipe was investigated recently [7], and the flow was found to be unstable at moderate Reynolds numbers. It should be noted that in all previous works, the axial characteristic lengths of the wall variation are of the same order as the pipe diameter, however, and much larger than the scale of a typical roughness. Therefore, the characteristic difference between the length scales of the roughness and of the pipe has not been taken into account in theoretical studies until now, and the problem: how small-scale wall variation induces instability in pipe flows, is thus still open.

One mechanism, referred to as mean flow instability hereafter, to sustain unstable disturbances in shear flows is when the mean flow profile mildly deviates from the stable basic flow profile, the flow may become unstable [8]. It has been found that the Hagen-Poiseuille profile modified by a small axisymmetric and axially invariant distortion was subjected to spatial instability, and the mode with one azimuthal period was the most prone to destabilization by an inviscid mechanism [9]. For parabolic profiles distorted by axisymmetric and nonaxisymmetric azimuthally periodic deviations, it was revealed that the corresponding instabilities might induce two different paths to transition [10]. Nevertheless, in previous studies of circular pipe flows, the mean flow instability can lead to streamwise

vortices and streaktype structures, but those profile distortions exist only when a prescribed volume force or pressure deviation is applied in the axial direction [9]. It is shown in this Letter how fine roughness affects the mean flow and consequently triggers instability.

The rough pipe is simulated by a circular pipe with fine surface corrugations and is described by cylindrical coordinates x^* , r^* , and ϕ^* , respectively. Its corrugation amplitude and wavelength are both much smaller than the average radius R_0 (see Fig. 1). The Reynolds number is defined as $Re = \frac{2R_0 U_0}{\nu}$, and the flow rate $Q = \pi R_0^2 U_0$. Using R_0 as length scale and U_0 as velocity scale, we obtain the dimensionless governing equations for the velocity field $\mathbf{u}(x, r, \phi, \tau)$ with components u, v, w in the x, r , and ϕ directions, respectively. The boundary conditions are no-slip on the pipe wall where $R(x) = 1 + \epsilon \sin(nx)$ and boundedness at the center line. ϵ is the relative roughness. For fine roughness, the corrugation wavelength $\delta = \frac{2\pi}{nR_0} = \frac{2\pi}{n} \ll 1$ is required. It is also assumed that $\epsilon \ll \delta$ or the shape factor $S = n\epsilon \ll 2\pi$, so the flow is nearly parallel both in the center region and near the corrugated wall.

In order to study the mean flow stability, one needs to solve the basic flow solutions $U(x, r)$ and $V(x, r)$ first. By scaling, it is easy to check that the inertia terms in axial momentum equation cannot be ignored when δ is not much larger than $Re\epsilon$. Hence, the Navier-Stokes equations for

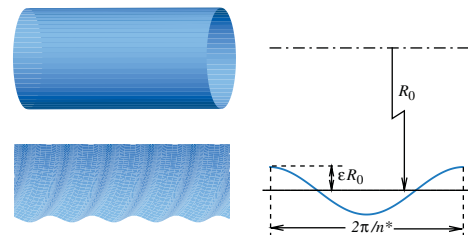


FIG. 1 (color). Sketch of the setup. The pipe surface has fine corrugations as $R_0[1 + \epsilon \sin(n^* x^*)]$, where $\epsilon \ll \frac{2\pi}{n^* R_0} \ll 1$.

the basic flow are simplified as

$$U \frac{\partial U}{\partial x} + V \frac{\partial U}{\partial r} = -\frac{\partial P}{\partial x} + \frac{2}{\text{Re}} \left(\frac{\partial^2 U}{\partial r^2} + \frac{1}{r} \frac{\partial U}{\partial r} \right) \quad (1)$$

$$\frac{\partial U}{\partial x} + \frac{1}{r} \frac{\partial(Vr)}{\partial r} = 0$$

with boundary conditions $U(x, R) = V(x, R) = 0$.

Since we are interested in the asymptotic behavior of fine roughness (e.g., the corrugation wavelength δ is third or fourth order smaller than the pipe diameter), it becomes a hard task to use numerical [7] or theoretical methods [3–5] to obtain such basic flow solution. Instead, we use an approximate solution of (1), which was solved with an integral method for converging-diverging tube [11] and is applicable for current model as $\epsilon \ll \delta$:

$$U(x, r) = \frac{2}{R^2} \left(1 - \frac{r^2}{R^2} \right) + \frac{\text{Re}}{R^3} \frac{dR}{dx} \left[\frac{8}{225} - \frac{8}{225} \frac{r^2}{R^2} - \frac{4}{15} \frac{r^3}{R^3} + \frac{4}{15} \frac{r^4}{R^4} \right]. \quad (2)$$

V can be calculated easily based on the continuity equation. When the pipe wall is smooth, $R(x) = 1$, the basic flow solution (2) reduces to the classical Hagen-Poiseuille flow solution. Since the corrugation wavelength $\delta \ll 1$, the axial length scale of basic flow structure described by (2) is much smaller than the average radius R_0 . The latter is the scale of typical structures (e.g., waves and axial vortices) observed in laminar-turbulent transitions. Therefore, it is interesting to find how these small-scale structures affect the mean flow field \hat{U} .

Mean Flows in practical circular pipes appear steady, axisymmetric, and parallel at low Reynolds numbers, or $\hat{U} \approx \hat{U}(r)$, so the governing equations for mean flow are reduced to

$$-\frac{\partial \hat{P}}{\partial x} + \frac{2}{\text{Re}} \left(\frac{\partial^2 \hat{U}}{\partial r^2} + \frac{1}{r} \frac{\partial \hat{U}}{\partial r} \right) = 0 \quad \hat{U}(1) = 0, \quad \frac{\partial \hat{U}}{\partial r} \Big|_{r=0} = 0. \quad (3)$$

Obviously, $\frac{\partial \hat{P}}{\partial x}$ is independent of x and is a constant for laminar smooth-pipe flows. In both the large-scale flow (mean flow) and the small-scale flow near roughness elements, the pressure terms in (1) and (3) must remain to balance the viscous terms and to maintain the flow rate. Therefore, the pressure term is the bridge to connect different axial-scale flows in a rough pipe. In this Letter, the mean pressure gradient is estimated with the basic flow solution by ignoring ϵ^2 and higher order terms without Re:

$$\frac{\partial \hat{P}}{\partial x} + \mathcal{C} = \frac{\partial \bar{P}}{\partial x} = \frac{2}{\text{Re}} \left(\frac{\partial^2 \bar{U}}{\partial r^2} + \frac{1}{r} \frac{\partial \bar{U}}{\partial r} \right) - \left(U \frac{\partial U}{\partial x} + V \frac{\partial U}{\partial r} \right) \approx -\frac{16}{\text{Re}} - \frac{\text{Re}}{2} (n\epsilon)^2 f(r),$$

where $f(r) = \frac{8}{225} r^2 (-40r^4 + 21r^3 + 60r^2 - 45r + 4)$. The constant \mathcal{C} is chosen to guarantee a fixed flow rate,

and the averaged value is defined as $\bar{\psi} = \frac{1}{\delta} \int_0^\delta \psi dx$. It is noted that the basic flow solution is axially periodic with wavelength δ . Consequently, the mean flow solution is solved from (3),

$$\hat{U} = 2(1 - r^2) - \left(\frac{\text{Re}}{2} S \right)^2 g(r), \quad (4)$$

where $g(r) = h(1)(1 - 2r^2) + h(r) + 4(r^2 - 1) \times \int_0^1 h(r) r dr$ and $h(r) = \int_0^r \frac{1}{r} \int_0^r f(r_1) r_1 dr_1 dr$. The first term on the RHS of (4) is just the Hagen-Poiseuille flow solution, and the second term embodies the nonlinear effect of the pipe-wall corrugation. To our knowledge, it is the first time to illustrate theoretically that how small-scale wall variation or fine roughness affects the mean velocity profile. It is also interesting to note that the mean flow is not affected by the relative roughness but by the Reynolds number and the shape factor $S = n\epsilon$, which divided by 2π is the ratio of the corrugation amplitude to its wavelength.

The mean flow stability analysis was carried out based on the mean flow solution (4). The form of rotating-symmetric disturbance to be considered is

$$\tilde{u}, \tilde{v}, \tilde{w}, \tilde{p} = \mathbb{R}[F(r), iG(r), H(r), J(r)] e^{i(m\phi + \alpha x - \omega \tau)}, \quad (5)$$

where the integer m and α are wave numbers in the azimuthal and the axial directions, and the imaginary part of the complex frequency ω determines the stability of the pipe flow to particular disturbance. The boundary conditions differ for different azimuthal wave numbers [12]:

$$\begin{aligned} m = 0, \quad & G(0) = F'(0) = G(1) = F(1) = 0; \\ m = 1, \quad & G(0) + H(0) = F(0) = H'(0) = F(1) \\ & = G(1) = H(1) = 0; \\ m \geq 2, \quad & F(0) = G(0) = H(0) = H'(0) = F(1) \\ & = G(1) = H(1) = 0. \end{aligned} \quad (6)$$

By substituting (6) into linearized Navier-Stokes equations, we obtain the governing equations of stability, which are resolved by a fourth-order finite difference scheme at uniformly distributed points in the r interval $[0, 1]$. A step size of $\Delta r = 1/200$ was used and checked by recomputing several points on the neutral curve with $\Delta r = 1/300$, and the new values agreed with the old ones to better than 0.5%. The solving method has been successfully used in previous studies [13,14].

According to stability analysis, the mean flow becomes unstable to a three-dimensional nonaxisymmetric traveling wave mode ($m = 1$) at moderate Reynolds numbers when the fine roughness exists. It is shown in Figs. 2(a) and 2(b) that the critical Reynolds number decreases with the increase of S . This is because larger shape factor S represents stronger nonparallel feature of the basic flow and larger mean flow modulation, which makes the flow more unstable. The mode with $m = 0$ may be unstable, but its critical Reynolds number is too high to be meaningful in

understanding the transition of rough pipe flows. In addition, different Reynolds numbers and shape factors are examined, and no unstable $m = 2$ and 3 modes are found, though the possibility of existence of unstable $m \geq 2$ mode is not excluded.

The mean velocity profiles at the critical states of $m = 1$ mode for $S = 0.006$ and 0.008 are shown in Fig. 2(c). Except for slight deviations from the parabolic profile, there are no inflection points on these curves, so the mean flow instability revealed in this Letter belongs to a viscous mechanism. By using small impulsive jets and push-pull disturbances from holes in pipe walls, it was found experimentally [15] that the disturbance amplitude threshold required to cause transition scaled as Re^{-1} (jets) and $\text{Re}^{-1.3}$ or $\text{Re}^{-1.5}$ (push-pull disturbance). Note that the introduced jets and disturbances are local ones and are not periodically distributed in the axial direction. According to the present fine-roughness model, the threshold of shape factor $S = n\epsilon$ scales as Re^{-2} as shown in Fig. 2(d), which should be examined by future experiments.

The disturbing flow patterns for $m = 1$ mode at critical state ($\text{Re} = 2581$ and $\alpha = 0.254$) as $S = 0.006$ are shown in Fig. 3. The main feature is a pair of regions with high or low axial velocity and a pair of axial narrow vortices, which are quite close to the wall. The amplitude of axial velocity component is about 7 times larger than other components, so there is strong longitudinal shear in the disturbing flow field. Another feature is that the disturbing velocity on the axis is not zero but a finite value with a rotating direction.

For basic flows, it has been shown numerically [7] that when the amplitude and wavelength of the roughness are comparable (e.g., in Nikuradze’s setup), the flow through

the pipe is “isolated” from the wall roughness by the surface of a streamtube, which deviates slightly and periodically from a straight tube with radius R_0 . Since the velocity on the streamtube is almost zero, as a first step, it may be simulated qualitatively by current corrugated pipe. In Nikuradze’s experiments, the roughness was simulated by uniform-size sand grains (the same aspect ratio or S), and the friction factor data almost collapse with each other at the beginning of transition though the relative roughness $\epsilon = R/R_0$ (the ratio of grain size to pipe radius) varies from $1/15$ to $1/507$. This experimental result agrees qualitatively with present theoretical prediction: it is the shape factor S , not the relative roughness ϵ , that determines the critical properties [e.g., the critical friction factor C_f as shown in Fig. 4(a)]. The quantitative relation between the critical Reynolds number and S still requires rigorous experimental tests.

Inspired by the analysis of the corrugation model and considering that S is almost a constant for sand grains, we assume that $C_f \text{Re} \sim \text{Re}^\gamma$ for flows through sand coated pipes at low Reynolds numbers. In addition, since sand grains have one single length scale ϵ , we assume that $C_f \text{Re} \sim \text{Re}^\xi \epsilon^\zeta$ at high Reynolds numbers. Naturally, we propose an empirical scaling form for the friction factor in Nikuradze’s experiments,

$$C_f \text{Re} = G(\text{Re}^\gamma + C_s \text{Re}^\xi \epsilon^\zeta), \quad (7)$$

where γ , ξ , and ζ are constants to be determined. C_s is determined to guarantee that all curves for different ϵ meet roughly at the same point shown by the arrow in Fig. 4(a). Note that no such a point exists in Moody’s chart because commercial pipes were used in those experiments, where

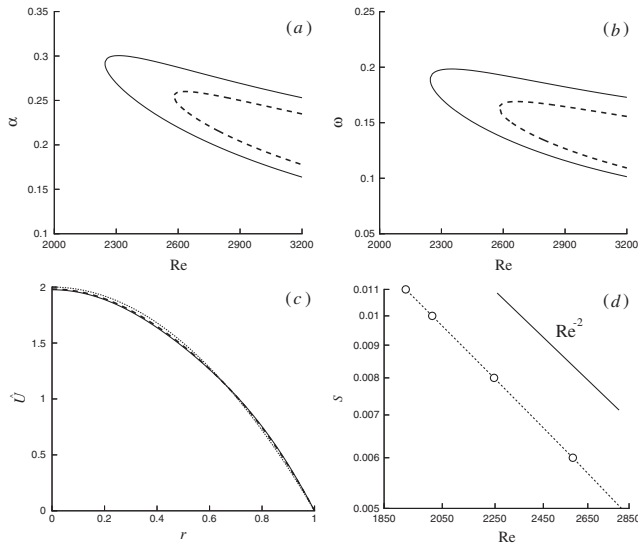


FIG. 2. Neutral curves (a), (b) and the mean velocity profiles at corresponding critical states (c) for $m = 1$ mode. The solid, thick dashed, and dotted lines are results for $S = 0.008, 0.006$, and 0 , respectively. (d) Critical shape factor S required to cause instability as a function of Reynolds number.

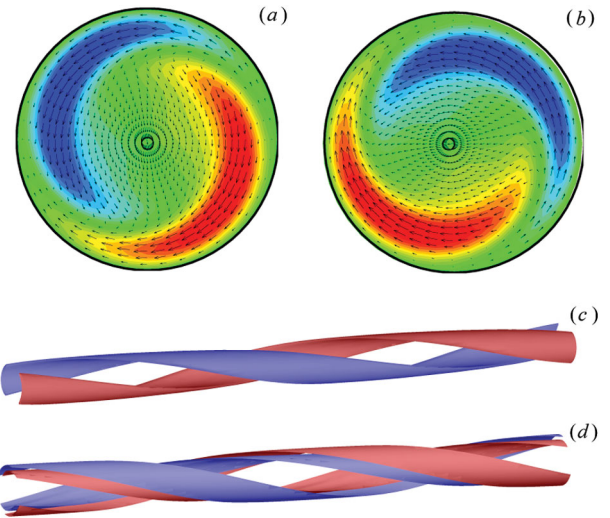


FIG. 3 (color). The disturbing flow fields of critical states at $S = 0.006$. The frames (a), (b) are separated with $\Delta x = \frac{\pi}{2\alpha}$, and the color contours indicate the values of disturbing axial velocity \bar{u} , which is about 7 times larger than other components. The isosurfaces of \bar{u} and axial vorticity are shown in (c) and (d), respectively.

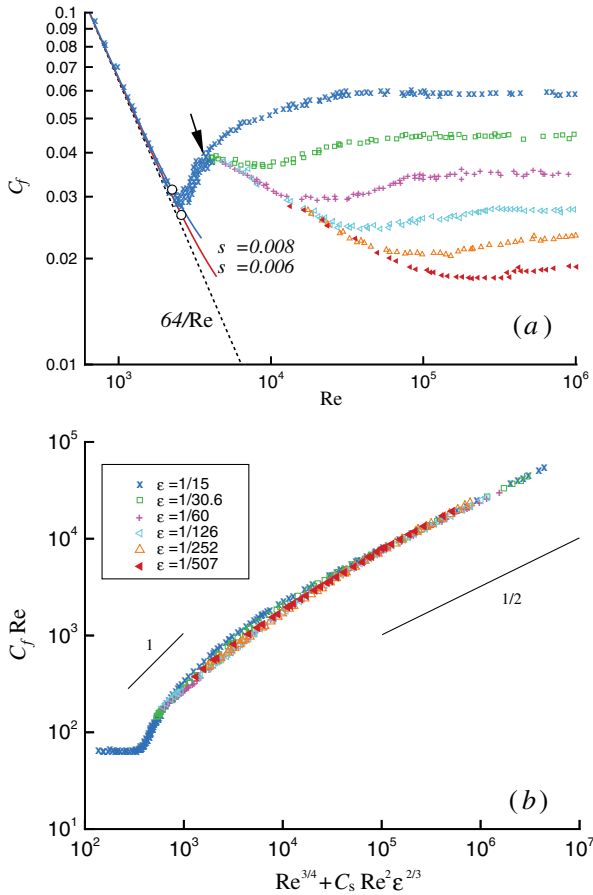


FIG. 4 (color). (a) Friction factor C_f as a function of Reynolds number. The red and blue lines satisfy $C_f Re = 64 + \frac{32}{1575} Re^2 S^2$ obtained from (4). The empty circles indicate the critical values for $m = 1$ mode. (b) Friction factor in experiments as reported by Nikuradze [2], scaled according to the text.

the roughness shape, unlike sand grains, varied with locations and pipe materials. Therefore, C_s reflects the shape character of roughness element and is referred as shape coefficient hereafter. In turbulence regime, it is easy to apply the method proposed by Goldenfeld [16] to find that the Blasius Law yields $\gamma = 3/4$ and the Strickler Law yields $\zeta/\xi = 1/3$. In order to test the scaling form (7), $\xi = 2$ is used and correspondingly $C_s = 3 \times 10^{-5}$ is determined. As shown in Fig. 4(b), all Nikuradze's data at different relative roughness ϵ collapse onto one single curve.

Friction factor C_f in rough pipes, as a mean property of turbulent flows, has been investigated with phenomenological theory of Kolmogórov [17] and empirical scaling laws [16]. Based on the analogy between turbulence and critical phenomenon, the latter showed that Nikuradze's data in turbulence regimes collapsed roughly on one curve when properly scaled. Different from these previous attempts of scaling, the curve shown in Fig. 4(b) not only includes the data between the Blasius and Strickler re-

gimes, but also includes the measurements in laminar and transitional regions. Although (7) is an empirical form, the data collapse suggests that a thorough understanding of the roughness-induced transition of pipe flows must include not only the relative roughness but also the shape configuration (e.g., C_s) of the fine-roughness element, whose effect has not been reported before. It is also shown that the data collapse is not rigorous in some regimes, reflecting uncertainties in the data and the possibility that C_s may be not a constant but a weak function of some fundamental parameters.

In conclusion, different from previous studies, this Letter constitutes the first bridge for pipe flow between the modulated velocity profile required by mean flow instability and its physical origin, which is the fine roughness in the present model. Since the current universal curve shown in Fig. 4(b) includes the whole range of Reynolds number, (7) is likely to be the simplest universal scaling form in the sense of being dependent of Reynolds number and the nature of the roughness of the pipe.

I acknowledge the valuable discussions with Fazle Hussain, Mingde Zhou, Friedrich H. Busse, and Zhensu She. This work has been supported by the NSFC (10922007) and (10921202).

*jjtao@pku.edu.cn

- [1] O. Reynolds, Proc. R. Soc. London **35**, 84 (1883).
- [2] J. Nikuradze, vDI Forschungsheft **361** (1933) [NACA Tech. Memo. **1292** (1950)].
- [3] J. M. Floryan, J. Fluid Mech. **482**, 17 (2003); Eur. J. Mech. B, Fluids **26**, 305 (2007).
- [4] J. Szumbarski and J. M. Floryan, J. Fluid Mech. **568**, 243 (2006).
- [5] M. Asai and J. M. Floryan, Eur. J. Mech. B, Fluids **25**, 971 (2006).
- [6] A. Lahbabi and H. Chang, Chem. Eng. Sci. **41**, 2487 (1986).
- [7] D. L. Cotrell, G. B. McFadden and B. J. Alder, Proc. Natl. Acad. Sci. U.S.A. **105**, 428 (2008).
- [8] A. E. Gill, J. Fluid Mech. **21**, 503 (1965).
- [9] M. I. Gavarini, A. Bottaro, and F. T. M. Nieuwstadt, J. Fluid Mech. **517**, 131 (2004).
- [10] G. Ben-Dov and J. Cohen, Phys. Rev. Lett. **98**, 064503; J. Fluid Mech. **588**, 189 (2007).
- [11] J. H. Forrester and D. F. Young, J. Biomech. **3**, 297 (1970).
- [12] G. K. Batchelor and A. E. Gill, J. Fluid Mech. **14**, 529 (1962).
- [13] J. Tao and F. Zhuang, Phys. Rev. E **62**, 7957 (2000).
- [14] J. Tao, P. Le Quéré, and S. Xin, J. Fluid Mech. **518**, 363 (2004).
- [15] J. Peixinho and T. Mullin, J. Fluid Mech. **582**, 169 (2007).
- [16] N. Goldenfeld, Phys. Rev. Lett. **96**, 044503 (2006).
- [17] G. Gioia and P. Chakraborty, Phys. Rev. Lett. **96**, 044502 (2006).